Cell separation technique in dilectrophoretic chip with bulk electrode

Ciprian Iliescu[*a], Francis E.H. Tay[a,b], Guolin Xu[a] and Liming Yu[b]

[a] Institute of Bioengineering and Nanotechnology, 31 Biopolis Way, The Nanos, Singapore 138669;
[b] Department of Mechanical Engineering, National University of Singapore, Singapore 117576

ABSTRACT

This paper presents a new technique for separation of two cell populations in a dielectrophoretic chip with bulk silicon electrode. A characteristic of the dielectrophoretic chip is its "sandwich" structure: glass/silicon/glass that generates a unique definition of the microfluidic channel with conductive walls (silicon) and isolating floor and ceiling (glass). The structure confers the opportunity to use the electrodes not only to generate a gradient of the electric field but also to generate a gradient of velocity of the fluid inside the channel. This interesting combination gives rise to a new solution for dielectrophoretic separation of two cell populations. The separation method consists of four steps. First, the microchannel is field with the cells mixture. Second, the cells are trapped in different locations of the microfluidic channel, the cell population which exhibits positive dielectrophoresis is trapped in the area where the distance between the electrodes is the minimum whilst, the other population that exhibit negative dielectrophoresis is trapped where the distance between electrodes is the maximum. In the next step, increasing the flow in the microchannel will result in an increased hydrodynamic force that sweeps the cells trapped by positive dielectrophoresis out of the chip. In the last step, the electric field is removed and the second population is sweep out and collected at the outlet. The device was tested for separation of dead yeast cells from live yeast cells. The paper presents analytical aspects of the separation method a comparative study between different electrode profiles and experimental results.

Keywords: dielectrophoretic chip, cells separation, hydrodynamic force, dielectrophoretic force

1. INTRODUCTION

In recent years, the development of miniaturized devices for the analysis and manipulation of cells or viruses is a fast growing field in microsystem technology. Such devices have many advantages such as: the reduction in size, low cost (mass production), portable and easy to be integrated. It has great potential for point-of-care diagnostics, surface-based biosensors, rapid cell, DNA analysis, etc. One of the great interests is the development of microfabricated dielectrophoresis (DEP) chip. It provides an effective way to separate and manipulate cells and/or particles automatically and quickly, which makes it possible for sample preparation.

DEP is a motion of dielectric particles caused by polarization effects in a non-uniform electric field. Many DEP devices have employed thin multilayer metal (usually between 100 nm and 1 μm-thick), deposited on a glass surface to form electrodes. Then the glass wafer is bonded to an insulating substrate such as glass [1], polycarbonate [2], Teflon gasket [3] or PDMS [4] to form the microchambers and microchannels. But such devices have some disadvantages: DEP force is confined in a region close to the thin electrode surfaces, there are dead volumes where the particle experiences no DEP force (the particles can not be manipulated) and there is electrochemical effect generated by double metallization (Ti/Pt or Cr/Au).

We proposed in the present paper a new method for cell/particle separation. The technique is based on the gradients of the dielectrophoretic force and the hydrodynamic force generated in the microfluidic channel with irregular shape of the channel walls, walls that act, in the same time, as electrodes of the dielectrophoretic device.

---

[*] ciliescu@ibn.a-star.edu.sg; phone: 65-68247137, fax 65-64789082, www.ibn.a-star.edu.sg

2. SEPARATION METHODS

Separation of particles or different types of cells is one of the main applications of the dielectrophoresis. Hughes [5] gives a brief description of separation methods using dielectrophoresis. These can be summarized as: flow separation, field flow fractionation, stepped flow separation, travel wave dielectrophoresis, and the ratcheting mechanism.

The flow separation method consists of a solution flowing with a particle suspension over an electrode array. When there are multiple populations that exhibit positive and negative dielectrophoresis, one population will be trapped near the electrode while the other one will be repelled into the center of the chamber to be subsequentially pushed by the flow towards the outlet. Flow separators have been reported and demonstrated in [6-8].

Another method uses a fluid velocity gradient to separate particles. Using an applied dielectrophoretic force field, different particles will be located at different regions within the fluid velocity gradient and will travel with different velocities. This separation method known as field-flow fraction and is presented in [9-12].

In [13] Markx et al describe a method that can be used for separation of bacteria, yeast and plant cells. The method uses castellated electrodes for cell trapping and two ports for outlet, one for inlet. Particles flow from the center of the array to one of the ports. When the electric field is applied positive and negative dielectrophoretic forces are experienced by each population of particles. Similar to field-flow fraction, when the liquid is pumped a hydrodynamic force is applied to the cells, and if this force is larger then the dielectrophoretic force the cells will be swept out. The populations can be separated and driven in opposite directions towards the two ports by selecting the correct frequency and electrical properties of the medium.

Traveling wave dielectrophoresis is another separation method. A traveling electric field is generated by interdigitated, parallel electrodes. The electrodes are usually connected in 3-4 periodic intervals with different phases (0°, 120° and 240° or 0°, 90°, 180° and 270°). Related work was reported by Huang et al [14] (separation of yeast cells according with size), Hughes et al [15] (separation by changing the frequency of the electric field) and by Fuhr et al [16] ("spiral electrode arrays").

The ratcheting mechanism has been reported in two configurations. The first system uses a "Christmas tree" electrode and, as source for particle motion - thermal motion (Brownian motion). Early work in this area was performed by Ajdari and Prost [17] and Rousselet et al [18]. Stacked ratchets are the second methods it consist in two pair of electrodes that are stack one over other. The populations are inserted between these electrodes and alternating the potential between upper and lower electrode moves particles.

3. PRINCIPLE OF SEQUENCIAL FIELD-FLOW SEPARATION METHOD WITH A DIELECTROPHORETIC CHIP WITH 3-D ELECTRODES

The objective of the design is to achieve efficient separation of particle populations. The efficiency is achieved by creating a structure where separation takes place over the entire cross-section of the fluidic flow. This ensures that particles flowing at any height within the channel are separated. The two distinct features of the separation structure are periodic fluidic dead volumes that are created by an undulating micro channel wall shape, and an extruded electrode design that exerts a dielectrophoretic force parallel to the channel floor and ceiling, and normal to the fluidic dead zones. A dielectrophoretic force that is parallel to the channel floor and ceiling ensures that there are no unnecessary friction forces on the particles to impede their motion and reduce the sorting efficiency. The force exerted on particles with different dielectric properties can be a positive or negative dielectrophoretic force. Correct selection of the operating frequency allows this difference to be used to separate the particle populations.

Sequential separation consists of four steps presented in Figure 1. Initially the channel is filled with the particle mixture (Figure 1a). At the optimal frequency, one population will experience a negative dielectrophoretic force that drives particles into the dead fluidic zones where they remain trapped (Figure 1b –zone B). Simultaneously the other

population will experience a positive dielectrophoretic force that focuses them in the region of the channel cross-section where the maximum fluid velocity occurs during flow (Figure 1b –zone A). After the particles have segregated themselves into the two regions within the channel, fresh buffer solution is pumped through the channel. The population that was focused at the centre of the channel where the velocity is greatest is swept out by the drag force exerted by the fluidic flow (Figure 1c). The population trapped in the fluidic dead zones remains trapped under flow or no-flow conditions. The dielectrophoretic force capturing the population in the dead zones is then reversed, and the captured population can be swept out (Figure 1d).
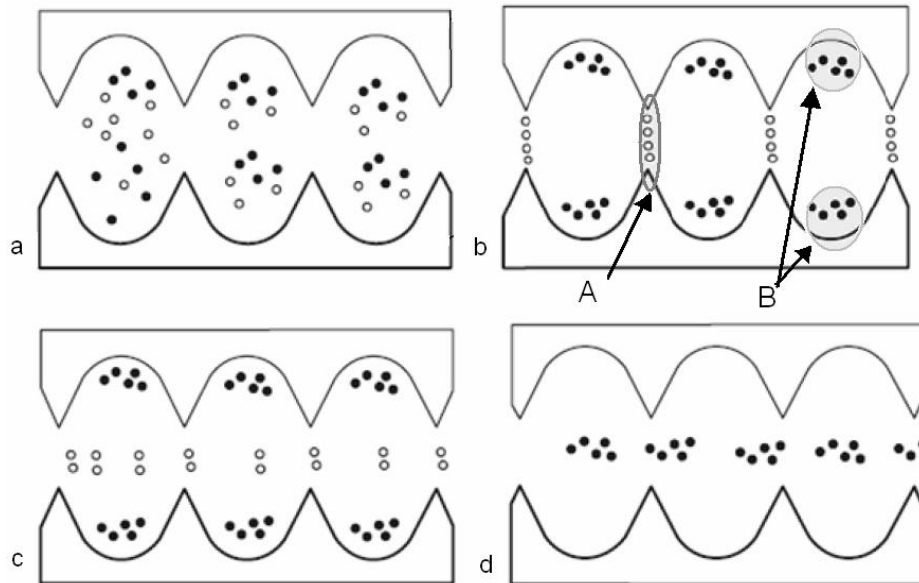

Figure 1: Separation method: a) insertion of the particles in the DEP chip, b) cells separation using positive and negative dielectrophoresis, c) removing the first population by increasing the velocity of the fluid, d) removing the electric field the second population will be released.

In the following section we will discuss the formation of the fluidic dead zones by numerical (ANSYS) simulation of different wall structures. We will then present the extruded electrode design using electric field analysis (Maxwell simulation) and analyze the dielectrophoretic force and the gradient of the electric field that are generated across the channel for different electrode designs. Finally we analyze the cumulative effect of dielectrophoretic and hydrodynamic forces for different electrode profiles.

4. THEORETICAL ANALYSIS AND SIMULATIONS

4.1 Hydrodynamic force

The flow of the fluid in the microchannel can play an important role in the separation performance of the dielectrophoretic device. In our special case the shape of the channel walls generates a specific velocity gradient in the fluid flowing in the microchannel that is essential for separation. Figure 2 shows an ANSYS simulation of the flow in microchannels defined by electrodes extruded walls with different geometries (semicircular, triangular and rectangular) with a minimal channel width of 100 μm and a maximal opening of 300 μm. The simulations were performed for a flow rate of 5×10^{-5} μl/s. These geometry leads to a huge gradient in the flow velocity between the maximum and minimum wall separation regions, neglecting the boundary layer values (which are zero by definition in the non-slip continuum model case). The low velocity regions will from here on be referred to as dead zones (let's approximate with the area where the fluid velocity is less than 10% of the average velocity in the centre of the channel). For this reason the hydrodynamic force (1) on the particles situated in the dead zones is more than one order lower than in the channel at its narrowest region. In equation (1):

$$F = 6\pi\,\eta\,r\,v \qquad (1)$$

η is the viscosity of the fluid, r is the radius of the particle and v is the velocity of the fluid. The hydrodynamic force is directly proportional to the velocity and radius of the particle. Decreasing the velocity by one order decreases the hydrodynamic force by one order.
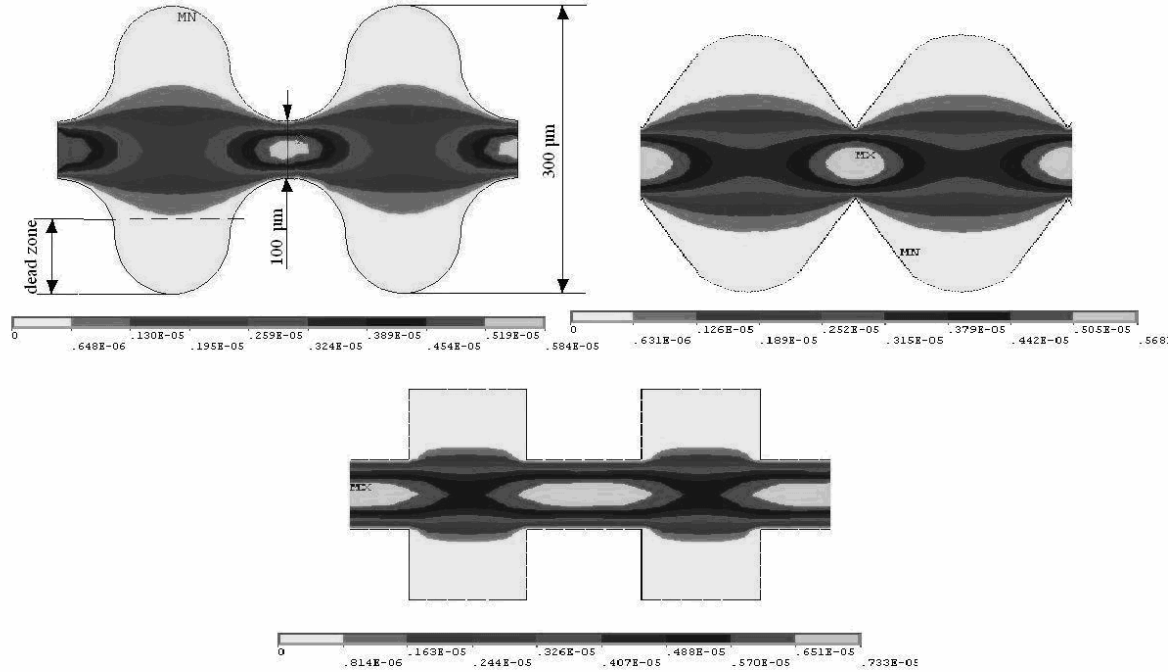

Figure 2: Velocity gradient of the fluid flow in microfluidic channel with semicircular, triangle and square electrodes.

The calculated hydrodynamic force for yeast cell, approximated by a sphere with a diameter of 7 μm, for a medium viscosity of 1×10^{-3} N.s/m^2 (water), and a velocity of 100 μm/s is 6.6×10^{-12} N.

4.2 Dielectrophoretic force

The dielectrophoretic force acting on a spherical particle with radius r is given by [19]:

$$F = 2\pi r^3 \varepsilon_m R_e[K(\omega)]\,\nabla E^2 \qquad (2)$$

where ε_m is the absolute permittivity of the suspending medium, ∇E is the local electric field (rms) intensity. Re[K(ω)] is the real part of the polarization factor, defined as:

$$K(\omega) = \left(\varepsilon_p^* - \varepsilon_m^*\right)/\left(\varepsilon_p^* + 2\varepsilon_m^*\right) \qquad (3)$$

And

$$\varepsilon^* = \varepsilon - j(\sigma/\omega) \qquad (4)$$

where ε_p^* and ε_m^* are the complex permittivity of the particle and medium respectively. The complex permittivity for a dielectric material can be described by its permittivity ε and conductivity σ, where ω is the angular frequency of the

applied electrical field E. Equations (2)–(4) show that a key condition for a dielectrophoretic force is that the complex permittivity of the particle ε_p^* is different from the complex permittivity of the medium ε_m^*. In most practical. cases this condition is satisfied.

In the expression of dielectrophoretic force (2), the term Re[K(ω)] (stands for "the real part of") plays an important role From relation (3), the definition of Re[K(ω)], the difference ε_p^* - ε_m^* can be positive or negative (Figure 3), giving either a positive or negative dielectrophoretic force. As a result, the movement of the particles towards the areas of high electric strength (positive dielectrophoresis) or low electric field strength (negative dielectrophoresis) is determined by the dielectric properties of the particles and medium. Particle populations that exhibit dielectrophoretic forces of opposite polarity can thus be separated in this way.
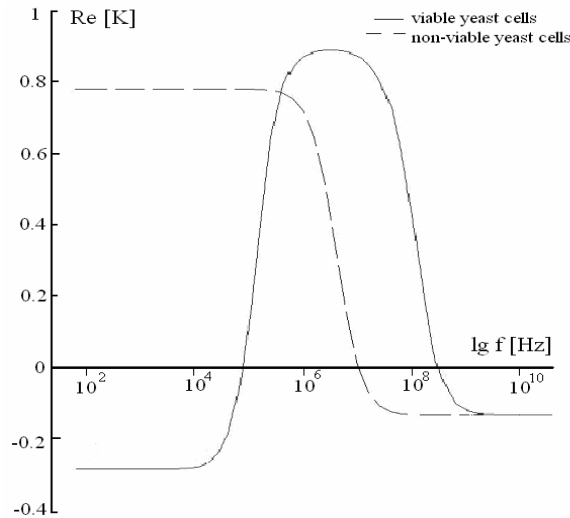
Figure 3: The frequency variation of the Re [K] for viable and non-viable yeast cells in a suspending medium with a conductivity of 1 mS/m.

The permeativity of the particle is strongly dependent of the frequency of the electric field generated. We consider for our experiment viable and non-viable yest cells. According with the model elaborated by Huang et al in [20] and applied also by Talary et al [21] and Hughes et al [15] will consider the values of 60, 6 and 50, respectively, for the relative permittivities of the yeast cell wall, cytoplasmic membrane and cell interior, respectively. For viable yeast cells the conductivities of the cell wall, membrane and interior were 14 mS/m, 0.25 μS/m and 0.2 S/m with thickness of cell wall, membrane of 0.22 μm and 8 nm respectively. Whereas for non-viable yeast the corresponding conductivity values were 1.5 mS/m, 160 μS/m and 7 mS/m, respectively (with the same dimention of the cell wall and membrane. Employing a cell wall thickness of 0.22 μm, a cell membrane thickness of 8 nm, and values of 7 and 6 μm for the radius of viable and non-viable yeast cells respectively, the frequency-dependency of the Re[K(ω)] were derived for suspending medium conductivities of 1 mS/m as shown in Figure 3. Can be noticed that for low freqencies up to 50 KHz viabile yest cells present a negative value of Re[K(ω)] which will be equivalent with a negative dielectrophoretic force while non-viabile yeast cell present a constant positive value. This range of frequeny will alowd separation of these populations. Another window of frequency can be between 10 MHz - 200 MHz where the situation is oposit: the viabile yeast cell will be trapped by positive dielectrophoresis while non-viable yeast cell will experience negative dielectrophoresis.

The simulation of the electric field is presented in Figure 4. The maximum electric field and the best gradient of the electric field can be achieved for the triangular shape. The electric field gradient and the dielectrophoretic force calculated for the same yeast cell with diameter of 6 μm positioned near the edge and in the center of the channel for all the three structure studied is presented in Table 1. The calculus was made for a permittivity of the medium of ε_m of 81 × 10^{-12} F/m and a Re[K(ω)] of 0.15 (maximum value for non-viable yeast cells) for a yeast cell suspended in aqueous solution with a conductivity of 1 mS/m.
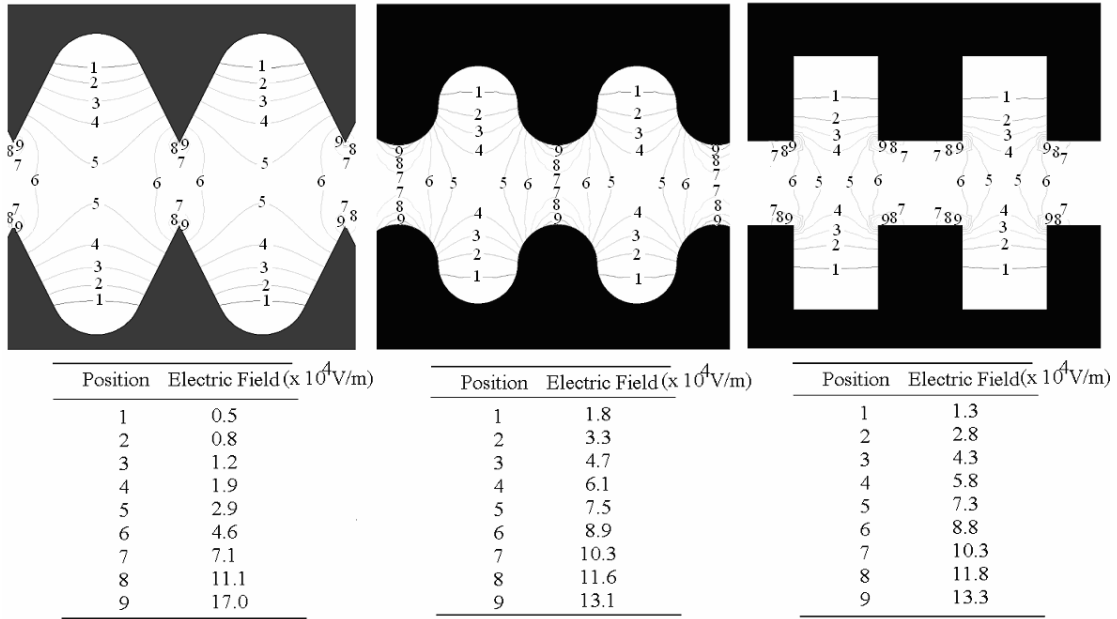
Position	Electric Field (x 10^4V/m)
1	0.5
2	0.8
3	1.2
4	1.9
5	2.9
6	4.6
7	7.1
8	11.1
9	17.0

Position	Electric Field (x 10^4V/m)
1	1.8
2	3.3
3	4.7
4	6.1
5	7.5
6	8.9
7	10.3
8	11.6
9	13.1

Position	Electric Field (x 10^4V/m)
1	1.3
2	2.8
3	4.3
4	5.8
5	7.3
6	8.8
7	10.3
8	11.8
9	13.3

Figure 4: Simulation of the electric field using Maxwell software for different design of electrodes.

A collate between the electric field generated in a dielectrophoretic structure with planar electrodes and a device with extruded electrodes is presented in Figure 5.Working with the extruded electrode design will generate a very uniform electric field in the vertical direction (Figure 5b). The uniformity of the electric field will determine a null dielectrophoretic force in direction perpendicular to electrode plane (electric field gradient is zero). A gradient of the electric field in vertical direction – characteristic of the planar electrode structure (Figure 5a)- will generate a dielectrophoretic force – F_{Z-DEP}- in this direction. For positive dielectrophoresis this force will be in the same direction with the gravity force and will increase the sedimentation and the trapping of the particle to the floor (where the hydrodynamic force is null). In addition to the dielectrophoretic force and hydrodynamic force, already mentioned, there are also other electro-hydrodynamic forces that act on the particles in a dielectrophoretic device. An analysis of these forces is presented by Ramos et al [22]. In our study these force term can be neglected.
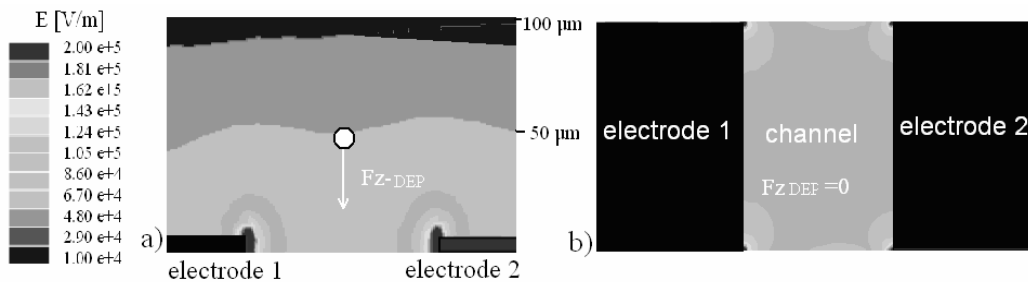

Figure 5: Simulation of the electric field in vertical plane (perpendicular to electrode) for a planar DEP structure (a) and extruded DEP structure (b)

Table 1 Electric field gradient and dielectrophoretic force

Electrode Shape	Position	Square	Semicircular	Triangular
Electric field gradient	Edge	$1.97\ 10^{14}$	$5.4\ 10^{13}$	$5.76\ 10^{13}$
[$\nabla E^2 (V^2/m^3)$]	Centre	$9\ 10^{12}$	$1.49\ 10^{12}$	$1.18\ 10^{12}$
Dielectrophoretic force	Edge	$1.24\ 10^{-11}$	$3.43\ 10^{-11}$	$1.18\ 10^{-11}$
[N]	Centre	$5.7\ 10^{-13}$	$9.4\ 10^{-14}$	$7.4\ 10^{-14}$

4.3 Electrode design consideration

The theoretical selection of electrod design require an analisys of positive and negative dileectrophoretic forces exhibit on particles (in our case yeast cells) and also the generated hydrodynamic force. Two zones are ananlised for each electrode tipe: one where the positive dielectrophoresis is experienced (in the area where the width of the channel is minimal) and the second where the opening of microfluidic channel is maximal (the zone where negative dielectrophoresis is generated).

For positive dielectrophoresis, the variation of dielectrophoretic force (for all above mentioned tipes of electrodes) and hydrodinamic force is presented in Figure 6. For a simplification only one curve was presented for hydrodynamic force.
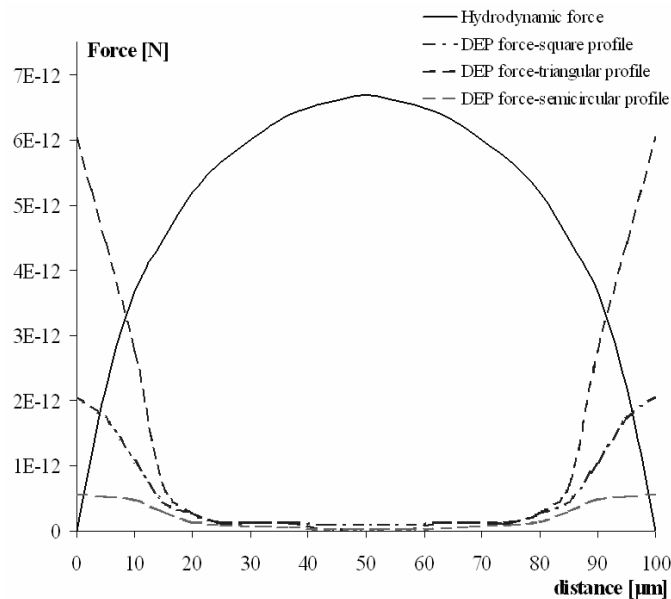
Figure 6: Variation of hydrodynamic force and positive dielectrophoretic force for different electrode profiles between electrodes tips for 100 µm channel width.

From Figure 6 we can observed that the triangular shape of the electrode gives a stronger dielectrophoretic force, with a maximal value near the tip of the electrode. The cells popululation which experience positive dielectrophoresis will be trapped between the tips of the electrodes, so the area where the particles will be in contact with the elctrodes (and at the same time with the microchannel walls) will be reduced. The zone where the modulus of dielectrophoretic force is biger then the modulus of hydrodinamic force is larger comparing with semicircular or square shape. But a comparation between the absolute values of dielectrophoretic and hydrodynamic forces is not relevant due to the fact that their direction is different. More relevant is to analyse the resulting force (composed from dielectrophoretic and hydrodynamic force). For this point of view we have three cases when the direction of the resulting force R is inside the electrode aria (Figure 7a) or is paralel with the triangle edge (Figure 7b) and in these cases the particle can not be released, it can be only move or role on along the edge of the electrode in the regions where the particle can slowly move to the regions where the hydrodynamic force is increased (high flow velocity) and where, also, the dielectrophoretic force present lower value. As a results the particle can be released. For the triangular electrode tipe can be expected small tulbulence in the vecinity of the tip that can improrve the releasing of the trapped particle. Improving of the releasing of the design can be achieved in two ways: by decreasing the angle of the triangle apex (in this way the probability that the direction of the resulting force to be outside the electrode area increase), by decreasing the dielectrophoretic force or by increasing the velocity of the fluid (with effect in incresing of the drag -hydrodinamic- force. By decreasing the angle the the profile in the dead regions will be similar with the squere electrode. Decreasing the dielectrophoretic force can be achieved by a carefull selection of some parameters like: conductivity of the solution (σ) or working frequency (that is equivalent with a smaller value of $Re[K(\omega)]$). Increasing the velocity can be performed between some experimental limits due to increasing of the velocity and force simultaneus in the area where negative dielectrophoresis is experienced. For the semicircular electrode the positive dielectrophoretic force presents a lower

value, but in this case the resulting force will keep the particle in the region situated near the electrode edge (where the velocity and also the drag force is reduced) -Figure 8a. For the square electrode the resulted foce will keep the particle in contact with the electrode edge – Figure 8b. Also in these cases a small positive dielectrophoretic force is recommended.
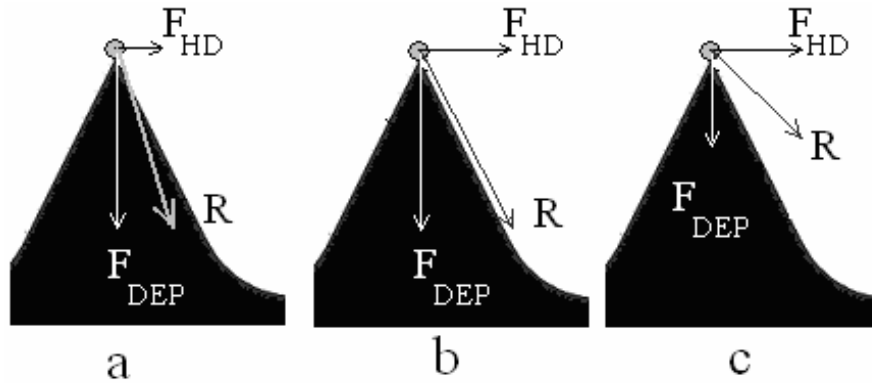

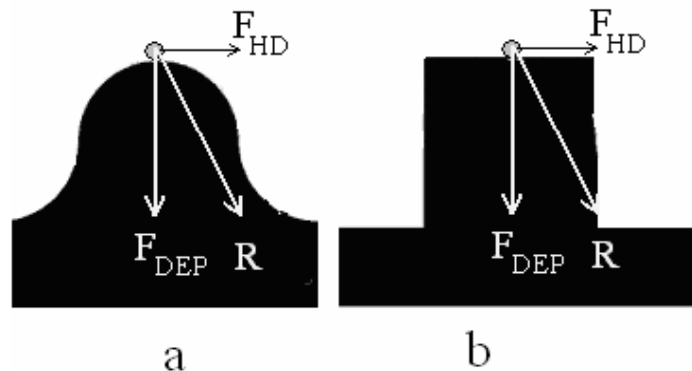Figure 7: Typical cases for triangular shape of electrode

Figure 8: Direction of the resulted force for semicircular and square shape of electrode.

For the population that experience negative dielectrophoresisthe variation of forcess is presented in Figure 9. The value of dilectrophoretic force is presented in absolute value. Can be observed that for the dead zone the dielectrophoretic force and also the hydrodynamic force is very weak. Moreover, as can be observed for the exemplification presented in Figure 10 for semicircular electrode, the resusltatnt force will keep the particle in the "dead zone" region.

The cells popululation which experience positive dielectrophoresis will be trapped between the tips of the electrodes, so the area where the particles will be in contact with the elctrodes (and at the same time with the microchannel walls) will be reduced. For the velocity point of view the maximal velocity is achieved in the channel with rectangular electrode, opposite to the semicircular and triangle structure the vertical plane that contain the maximal velocity value is not identical with the plane were most of the population is trapped by positive dielectrophoresis. For the rectangular design this plane is on the electrode corners. For the rectangular shape we notice turbulence in the "dead zone" (Figure 11). This turbulence can reduce the efect of the dilectrophoretic force exhibit on the population that experience negative dielectrophoresis, so the separation process can be affected.
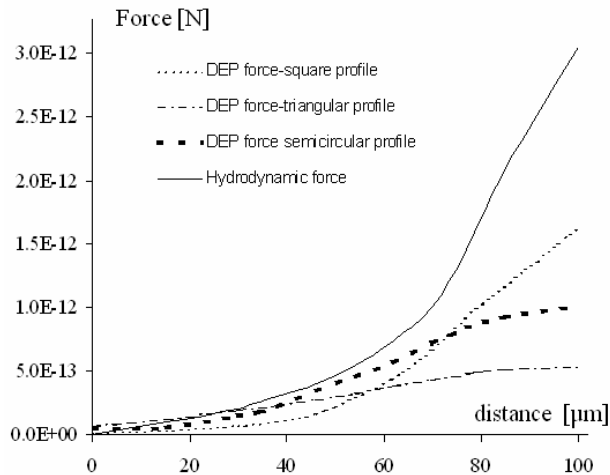
Figure 9: Variation of hydrodynamic force and positive dielectrophoretic force (different electrode profiles) for population that experience negative dielectrophoresis up to 100 μm distance for the channel wall.
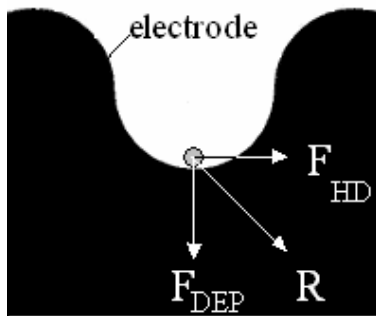

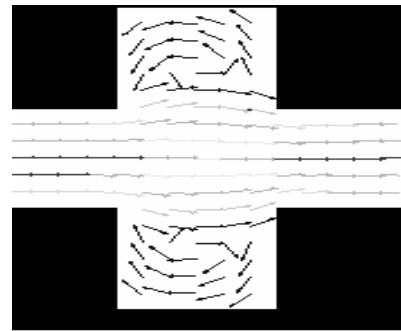Figure 10: Resulted force in the wheel

Figure 11: Vectorial simulation of the flowing in microfluidic channel

5. DEVICE DESCRIPTION AND FABRICATION

The separation method proposed in this paper is based on a dielectrophoretic chip with 3-D electrodes. We described the fabrication process of the device and its application to yeast cell concentration in [23]. An improved version of this chip is presented in Figure 12. As can be observed, the thick electrodes made from bulk silicon are sandwiched between two glass dies. The electrodes surface forms the walls of the microfluidic channels and the glass die form the ceiling and the floor of the microchannels. Via-holes were created in the bottom glass die and a metallization connects the electrodes to the contact pads. The inlet and outlet connections to the microfluidic channels are on the lateral sides of the chip and the sample is injected through classical syringe needles with a diameter of 0.41 mm.

The fabrication process presented in Figure 13 is an improved version of the process developed by us in [23]. A 4" conductive silicon wafer with a resistivity of 0.005-0.01 Ωcm, 300 μm thick, was anodically bonded to a glass wafer (Corning 7740) at 350°C with an applied voltage of 1000V for 15 minutes (Figure 13a). The patterning of electrodes was carried out with a deep RIE (Bosch process) in SF_6/C_4F_8 through a photoresist and silicon oxide mask (Figure 13b). A SEM picture with the patterning of the silicon is presented in Figure 14. A second wafer-to-wafer bonding process was performed using SU8-5 photoresist that was imprinted from a dummy silicon wafer to the top part of the electrode and then bonded at 150°C for 30 minutes with a applied pressure of 500 N (Figure 13c). Previous in the top glass wafer channel with a width of 400 μm and a depth of 200 μm was etched using a amorphous silicon mask in a HF 49%/HCl 37% solution (10/1). The bottom glass wafer was thinned up to 100 μm by wet etching in the same solution (Figure 13d). The uniformity of the process was in an acceptable rage (5%). The roughness (R_a) of the generated surface after the wet etching process was 10 nm. Via holes were created by wet etching in the same solution through a Cr/Au (50 nm/1 μm) mask – Figure 13e. After removing the mask another wet etching process of 1.5 minutes (equivalent to a

depth etch of 10 μm) was performed mainly to remove the sharpness of the edges and also to remove the non-uniform effects of the wet etching process. During the via-holes etching the etch-stop process cannot be realized due to the small size of the mask and the large depth of etching. In this way the risk of metallization step coverage issues over a sharp edge is eliminated. The metallization was performed using the same Cr/Au deposition. The photoresist AZ4620 (Clariant) was applied using and an optimized spray-coating process (Figure 13f). The fabricated device is presented in Figure 14.
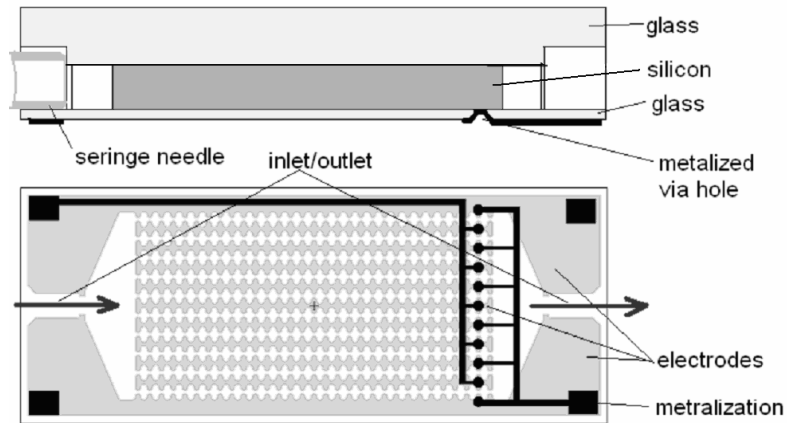

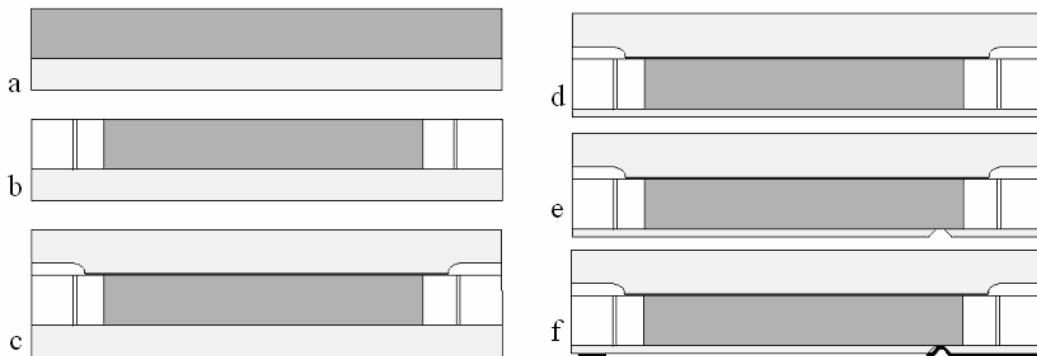Figure 12: Schematic drawing of the DEP chip

Figure 13 Fabrication process: a) anodic bonding, b) deep RIE process, c) SU8 bonding, d) glass thinning, e) via holes etching, f) metallization.
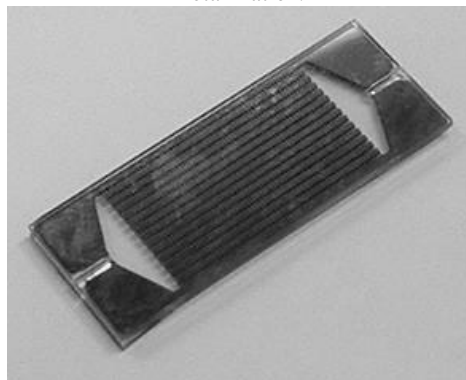

Figure 14: DEP device for cell separation

5. TESTING

For testing of the system performance two populations of live yest cells and dead yest cells were used. 100 mg of yeast, 100 mg of sugar and 2 ml DI water were incubated in an Eppendorf tube at 37^OC for 2 h. The cells were then concentrated by centrifugation at 1000 rpm for 1 min. The supernatant solution was removed and the cell pellet was washed by adding 2 ml of DI water into the tube. The centrifugation and washing process was repeated three times. The cell culture was divided in two and one population was boiled for few second in 5 ml DI water (dead cells). Then the cells was recollected by centrifugation. Both populations were mixed and resuspended in the separation buffer, which was a mixture of phosphate buffered saline (PBS) and DI water. The conductivity of the separation buffer was adjusted to about 1 mS/cm$_{-1}$ using NaOH. The final concentration the cells was 1×10^7cells/ml. A function generator and a linear amplifier were used for drive signal generation of the dielectrophoretic chip. Prior to injecting the cell suspension into the device, the protocol was to assure that the function generator and amplifier were powered on but their outputs were set to the minimum. This was to prevent the generation of bubbles inside the channel by electrolysis. The suspension with cell populations was injected into the chip and another buffer solution was prepared for removing of the population that will be trapped.

The drive signal was increased from 0 to 25 V peak to peak gradually. The signal frequency was anywhere in the range of 20 kHz to 100 kHz. The result of the testing are presented in Figure 15, where the main steps of the separation technique can be observed: flowing the cell population into the channel- Figure 15a, separation of the cell populations – Figure 15b and removing the population that express positive DEP forces –Figure 15c.
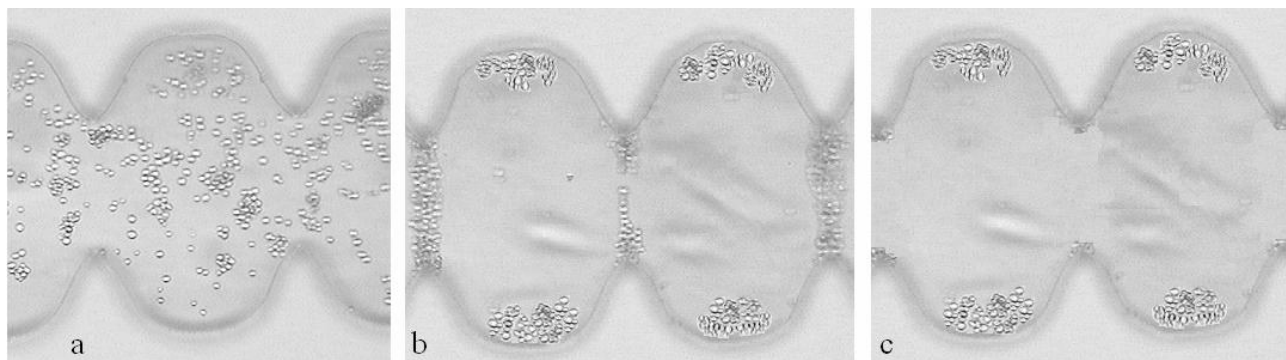

Figure 15: Main steps of the separation technique

6. CONCLUSIONS

A new sequential field-flow separation method in a dielectrophoretic chip with volumic electrodes is presented. A characteristic of the dielectrophoretic device presented in the paper is that the geometry of the electrodes defined also the geometry of the microfluidic channel. The methods successfully use the variation of the width of the microfluidic channel required by the necessity of gradient of the electric field generation to remove the population trapped by positive dielectrophoresis, while the second population remained trapped in the velocity "dead zone" of the microfluidic channel. The removing of the electric field will give the opportunity to the second population to be collected at the outlet.

ACKNOWLEDGEMENT

REFERENCES

1. Q. Ramadan, V. Samper and Z. Liang, *Microfluidic DNA sample preparation by dielectrophoresis and electroporation*, Proc. Eurosensors '02, 537-540, 2002.
2. Y. Huang, J.M. Yang and P.J. Hopkins, *Separation of simulants of biological warfare agents from blood by a miniaturized dielectrophoresis device*, Biomed. Microdevices 5/3, 217-225, 2003.
3. J.M. Yang, Y. Huang and X.B. Wang, *Cell separation on microfabricated electrodes using dielectroporetic/gravitational field-flow fractionation*, Anal. Chem. 71 (), 911-918, 1999.
4. Y.C. Lin, M. Li, C.S. Fan and L.W. Wu, *A microchip for electroporation of primary endothelial cells*, Sensors & Actuators A 108, 12-19, 2003.
5. M.P. Hughes, *Strategies for dielectrophoretic separation in laboratory-on-a-chip systems*, Electrophoresis, 23/16, 2569-2582, 2002.
6. H. Morgan, A.G. Izquierdo, D. Bakewell, N.G. Green and A. Ramos, *The dielectrophoretic and traveling wave forces for interdigitated electrode arrays: Analytical solution using Fourier series*, J. Phys. D: Appl. Phys., 34, 1553-1561, 2001
7. R. Pethig, J.P.H. Burt, A. Parton, N. Rizvi, M.S. Talary and J.A. Tame, *Development of biofactory-on-a-chip technology using excimer laser micromachining*, J. Micromech. Microeng. 8, 57-63, 1998.
8. M. Stephens, M.S. Talary, R. Pethig, A.K. Burnett and K.I. Mills, *The dielectrophoresis enrichment of CD34+ cells from peripherical blood steam cell harvests*, Bone Marrow Transplantation, 18, 777-782. 1996
9. G.H. Markx, R. Pethig and J. Rousselet, *The dielectrophoretic levitation of latex beads, with reference to field-flow fractionation*, J. Phys. D: Appl. Phys., 30, 2470–2477, 1997.
10. X.B. Wang, J. Vykoukal, F.F. Becker and P.R.C. Gascoyne, *Separation of polystyrene microbeads using dielectrophoretic/gravitational field-flow-fractionation*, Biophys. J., 74,/5, 2689–2701, 1998.
11. T. Müller, T. Schnelle, G. Gradl, S.G. Shirley and G. Fuhr, *Microdevice for cell and particle separation using dielectrophoretic field-flow fractionation*, J. Liquid Chromatog. Relat. Technol., 23/ 1, 47–59, 2000.
12. J. Yang, Y. Huang, X.B. Wang, F.F. Becker and P.R.C. Gascoyne, *Dielectric properties of human leukocyte subpopulations determined by electrorotation as a cell separation criterion*, Biophys. J., 76, pp. 3307–3314, 1999.
13. G.H. Markx and R. Pethig, *Dielectrophoretic separation of cells: Continuous separation*, Biotechnol. Bioeng., 45, 337–343, 1995.
14. Y. Huang, J.A. Tame, and R. Pethig, *Electrokinetic behavior of colloidal particles in traveling electric fields: studies using yeast cells*, J. Phys. D: Appl. Phys., 26, 1528–1535, 1993.
15. M.P. Hughes, R. Pethig and X.B. Wang, *Dielectrophoretic forces on particles in traveling electric fields*, J. Phys. D: Appl. Phys., 29, 474–482, 1996.
16. G. Fuhr, S. Fiedler, T. Müller, T. Schnelle, H. Glasser, T. Lis and B. Wagner, *Particle micromanipulator consisting of two orthogonal channels with traveling-wave electrode structures*, Sens. Actuators A, , 41–42, 230-239,1994
17. A. Ajdari and J. Prost, C. R. Acad. Sci. Paris, 315, 1635-1642, 1992
18. J. Rousselet, L. Salome, A. Ajdari, J. Prost, *Directional motion of Brownian particles induced by a periodic asymmetric potential*, Nature, 370, 446–448, 1994.
19. T.B. Jones, *Electromechanicas of particle*, Cambridge University Press, 1995.
20. Y. Huang, R. Hölzel, R. Pethig and X.B. Wang, *Differences in the AC electrodynamics of viable and nonviable yeast cells determined through combined dielectrophoresis and electrorotation studies*, Phys. Med. Biol., 37/ 7, 1499–1517, 1992.
21. M.S. Talary, J.P.H. Burt, J.A. Tame and R. Pethig, 1996, *Electromanipulation and separation of cells using travelling electric fields*, J. Phys. D: Appl. Phys., 29, 2198-2203, 1996.
22. A. Ramos, H. Morgan, N.G. Green and A. Castellannos, *AC electrokinetics: a review of forces in microelectrode structures*, J. Phys. D: Appl. Phys., 31, 2338-2343, 1998,
23. C. Iliescu, G. Xu, V. Samper, F.E.H. Tay, *Fabrication of a Dielectrophoretic Chip with 3D Silicon Electrodes*, J. Micromech. Microeng., 15/3, 494-500, 2005.
24. C. Iliescu, J.M. Miao, and F.E.H. Tay, *Stress Control in Masking Layers for Deep Wet Micromachining of Pyrex Glass*, Sens. and Act. A, 117/2, 286-292, 2005.